

# Wavelet analysis for detecting anisotropy in point patterns

Rosenberg, Michael S.

School of Life Sciences, P.O. Box 874501, Arizona State University, Tempe, AZ 85287-4501, USA;  
Fax +1 480 965 6899; E-mail msr@asu.edu

**Abstract.** Although many methods have been proposed for analysing point locations for spatial pattern, previous methods have concentrated on clumping and spacing. The study of anisotropy (changes in spatial pattern with direction) in point patterns has been limited by lack of methods explicitly designed for these data and this purpose; researchers have been constrained to choosing arbitrary test directions or converting their data into quadrat counts and using methods designed for continuously distributed data. Wavelet analysis, a booming approach to studying spatial pattern, widely used in mathematics and physics for signal analysis, has started to make its way into the ecological literature. A simple adaptation of wavelet analysis is proposed for the detection of anisotropy in point patterns. The method is illustrated with both simulated and field data. This approach can easily be used for both global and local spatial analysis.

**Keywords:** *Ambrosia dumosa*; Directional pattern; Global analysis; Isotropy; Joshua Tree National Park; Local analysis; Spatial analysis.

## Introduction

Point locations are common data in ecology, including such diverse phenomena as a population of trees or bushes, crustacean burrows, or human settlements. Numerous methods have been proposed to analyse spatial point patterns (e.g. Ripley 1976, 1977, 1979; Diggle 1983; Upton & Fingleton 1985; Perry 1995; Muggleston & Renshaw 1996; Perry et al. 1999); most focus on the determination of whether the points are clumped, regularly arranged, or randomly distributed through space. One aspect of point patterns that has received relatively little attention is the analysis of anisotropy. Anisotropy (or directionality) is the condition where different spatial patterns are found in different cardinal directions; most spatial analyses assume isotropy or are omnidirectional. While numerous methods have been developed to detect anisotropy in categorical (nominal) and continuously distributed data (Oden & Sokal 1986; Isaaks & Srivastava 1989; Falsetti & Sokal 1993; Simon 1997; Dale 1999; Rosenberg 2000), little has been done to study anisotropy in point patterns.

Analysis of anisotropy has tended to follow two general approaches. In the first, the points are turned

into quadrat counts by overlaying a grid across the extent of the study; the counts surface may then be analysed using standard anisotropic techniques for surfaces such as angular correlation (Simon 1997) or directional correlograms (Oden & Sokal 1986; Rosenberg 2000). While this approach can certainly work, it may also have limited power and will be very dependent on arbitrary choices of quadrat size and number. In the second approach, a standard point pattern method, e.g. Ripley's  $K$ , is calculated only for points related to each other by a specific direction (Dale 1999). This is repeated for different directions and the results are compared to see if different directions lead to different spatial patterns. A related approach, using the template concept of spatial analysis (Dale et al. 2002), is to use oblong, rather than symmetric, templates (i.e., calculate Ripley's  $K$  using ovals rather than circles). The problem with the latter approaches is that they do not determine directions of pattern; they can only be used to test for patterns in *a priori* specified directions. Muggleston & Renshaw (1996) discuss a method of determining anisotropy in point patterns as part of two-dimensional spectral analysis, but the complications inherent in spectral analysis (particularly for more than one dimension) appear to have discouraged ecologists from making use of these methods (Haining 1982; Franklin et al. 1985; Muggleston & Renshaw 1996).

The purpose of this paper is to introduce an adaptation of wavelet analysis to construct a specific method for determining anisotropic point patterns.

## Methods

To start, consider the question of anisotropy relative to a single observed point within the data set. The question can be asked whether the remaining observed points are found more often in certain cardinal directions than others. This question can be repeated using every observed point as a fixed focal point and examining the distribution of the remaining points relative to each focal point. For a specific focal point, the space around it is first divided into angular sectors (Fig. 1); for these purposes 360 1°-sectors are used, starting with due

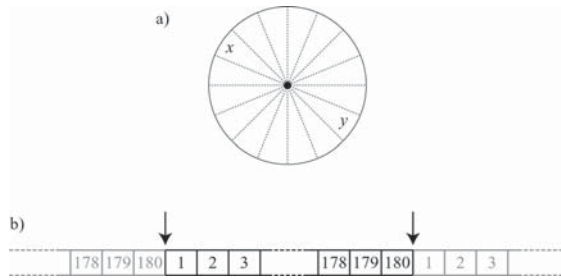


**Fig. 1.** Transformation of angular sectors into a transect. **a.** Division of space around a point into angular sectors. Sectors  $x$  and  $y$  are separated by  $180^\circ$  and are summed together. **b.** The transect created from the sectors; because the transect is circular, sectors 1 and 180 are adjacent, as indicated by the arrows.

east as  $0^\circ$ , and proceeding counter-clockwise (as in Falsetti & Sokal 1993; Rosenberg 2000). Then the number of points within the study area that fall into each sector are counted. However, we are not generally interested in trying to distinguish north to south from south to north because the ‘direction’ of pattern is arbitrary without additional information on a process; instead we wish to know whether the spatial pattern in a north-south bearing is similar or different from that of another bearing. Therefore, counts from opposite sectors are combined, to produce 180 sector counts (Fig. 1). These sectors can be considered a circular transect, with one end looping around to the other. A particularly interesting method by which to analyse a transect is wavelet analysis.

Wavelet analysis has been heavily used in mathematics and engineering for signal analysis and data compression (e.g. Chui 1992; Donoho 1993; Strang 1994; Greiner et al. 1996), but has had limited (although expanding) use in ecology (Bradshaw & Spies 1992; Bradshaw & McIntosh 1994; Dale & Mah 1998; Nakken 1999; Perry et al. 2002). For our purposes, a wavelet function  $g(x)$  is a scalable windowing function; one way to picture wavelet analysis is that the wavelet function describes a template (Dale et al. 2002) which can be scaled to a desired size, then slid along the transect. When the template fits the observed data well the value of the wavelet transform at that position is high, when it does not, the value is low (this is well illustrated in Fig. 1 of Dale & Mah 1998). There are many possible wavelet functions to choose for an analysis (Daubechies et al. 1986; Daubechies 1988, 1993; Dale & Mah 1998). One simple wavelet function is known as the French Top Hat; this is a three-term function with a discrete square template. Its formula (Dale & Mah 1998) is:

$$g(x) = \begin{cases} -1 & \text{if } 1/2 < |x| < 3/2 \\ 2 & \text{if } |x| < 1/2 \\ 0 & \text{otherwise} \end{cases} \quad (1)$$

Although the choice of a specific wavelet function will often make little difference in the interpretation of results, three-term functions are often more accurate predictors of scale than similar two-term functions, for the same reasons that three-term local quadrat variance tends to be more accurate than two-term local quadrat variance (Dale 1999).

The wavelet transform at position  $x_i$  for scale  $b_k$  is equal to

$$W(b_k, x_i) = \frac{1}{b_k} \sum_{j=1}^n y(x_j) g\left(\frac{x_j - x_i}{b_k}\right) \quad (2)$$

where  $y(x)$  is the value of the data at position  $x$ ,  $n$  is the number of observations along the transect, and  $b_k$  is the scale of analysis (a discrete distance over which the wavelet template is stretched). The overall variance for a given analysis scale,  $b_k$  is given as

$$V(b_k) = \frac{1}{n} \sum_{i=1}^n W^2(b_k, x_i) \quad (3)$$

or the average of the squared wavelet transforms at all positions for that scale.  $V(b_k)$  will be maximal when the wavelet template stretched to that scale best fits the data; put another way,  $V(b_k)$  is maximized when  $b_k$  is equal to the average size of patches and gaps. Similarly, the overall variance for a given position,  $x_i$ , is

$$P(x_i) = \frac{1}{m} \sum_{k=1}^m W^2(b_k, x_i) \quad (4)$$

or the average of the squared wavelet transform over all scales ( $m$  is the total number of discrete measured scales).  $P(x_i)$  is maximized when wavelet templates centred at location  $x_i$  fit the data better than other locations. A typical wavelet analysis in ecology produces a plot of each of these functions: variance as a function of position  $P(x_i)$ , variance as a function of scale  $V(b_k)$ , and a surface of the wavelet transform as a function of scale and position  $W(b_k, x_i)$  (Dale & Mah 1998; Rosenberg 2001; Perry et al. 2002). A simple example is illustrated in Dale & Mah (1998) and Rosenberg (2001).

Returning to the angular sectors, we can calculate the wavelet transformation on these sectors by treating them as a circular transect (remembering that the ends of the transect are adjacent, Fig. 1). In this case, the position  $x_i$  represents the direction in which each bearing points ( $\theta$  (east-west, northeast-southwest, etc.) and the scale  $b_k$  is equal to the angular width of the sector  $\varpi$  ( $1^\circ$ ,  $2^\circ$ ,  $3^\circ$ , etc.). This analysis is based on the division of space into sectors based on a single fixed focal point, treating the remaining points as random; to estimate the global spatial pattern the average values of  $W(\varpi_k, \theta_i)$ ,

$V(\varpi_k)$ , and  $P(\theta_i)$  are calculated across the entire set of observed points, using each as the fixed focal point. Thus we use the observed data points to centre each wavelet analysis, much like second-order analyses such as Ripley's  $K$  (Ripley 1976) use circles centred on observed data points. This strategy was chosen, rather than the alternative of foci being data independent, because the goal of the analysis is to study the directional relationship among the observed points and not between the observed points and arbitrary positions within the study plot.

With a standard transect, we are generally most interested in  $V(b_k)$ , the relationship between variance and scale, since this indicates the average size of patches and gaps across the transect. This aspect of wavelet analysis is extremely similar to well known quadrat variance methods such as two- and three-term local quadrat variances (TTLQV and 3TLQV) (Hill 1973; Dale & Mah 1998). In the angular wavelet analysis, however, we are much more interested in  $P(\theta_i)$ . Peaks in this plot indicate the angle at which maximal variance was obtained; this is the direction in which most of the points can be found.  $V(\varpi_k)$  and  $W(\varpi_k, \theta_i)$  are less interesting in this analysis because  $\varpi$  represents the angular breadth of the sectors (a somewhat meaningless measure), although one can imagine circumstances where analysis of  $\varpi_k$  might be used to describe the breadth of repeating radial patterns.

One immediate complication is the shape of the study area. For any non-circular area, there is a potential directional bias in the sector counts, even for random point patterns. For example, in a square study area, for any focal point within the area, sectors pointing along the diagonals will contain more area than sectors pointing directly to a side (Fig. 2a), thus, by random chance there should be more points found in the diagonal directions than parallel to the sides. This can be corrected by converting the sector counts into a density measure (counts per area); for simplicity sake, each sector count is divided by the sum of the squared distances of the focal point to the edges of the study area along the angular bisector of the sector  $r_1^2 + r_2^2$  (the dotted lines in Fig. 2a). This sum is an adequate proxy of the area encompassed by the sector, in so far as that we assume the sector can be represented by a pair of pie-shaped sections of a circle (with the lengths of the perpendicular bisector from the focal point to the two edges representing the radius of each pie,  $r_1$  and  $r_2$ ) and noting that the actual area for a pair of sectors of given angular breadth  $\varpi$  (measured in radians) is  $\varpi\pi r_1^2/2\pi + \varpi\pi r_2^2/2\pi$ . Because the  $\pi$ 's cancel out and  $\varpi/2$  is constant for every sector for all possible focal points, they can be dropped leaving  $r_1^2 + r_2^2$  for computational simplicity. Unfortunately this correction itself can cause a problem when multiple points are located in a corner of the plot (Fig.

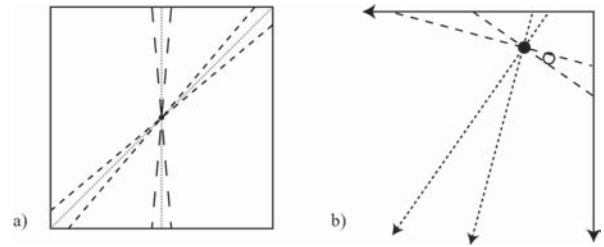


**Fig. 2.** Illustration of the problems of study area shape. **a.** Dashed lines demarcate two sectors; the dotted lines indicate the angular bisectors of each sector. The diagonal sector contains more area than the vertical sector. **b.** A small corner of a larger plot; the sector containing the open point will have abnormally high weight due to the relatively small area it encompasses.

2b). The area encompassed by sectors roughly perpendicular to the bisector of the corner (Fig. 2b) is extremely small relative to the area of sectors generated from the centre of the plot or which point into the corner. If there happens to be a second point in the corner, this count is given extremely high weight due to the tiny area and may result in a phantom peak. This problem may be even more serious with plots of irregular geometry. Since this corner problem is essentially an edge effect (Haase 1995), an obvious solution is to only use points located toward the centre of the plot as foci.

In order to separate true patterns from random fluctuations, the significance of the wavelet analysis can be determined through a Monte Carlo simulation, wherein one simulates random point patterns containing the same number of points (in the same shaped plot) as in the observed data. This procedure is repeated many times, and the distribution of the  $P(\theta_i)$  values from the simulated random patterns are used to judge the observed  $P(\theta_i)$  values. Because our null hypothesis is isotropy, a random pattern should be expected to have the same  $P(\theta_i)$  for all possible directions. We can therefore calculate the simulation distribution over not only multiple randomization replicates but also over all  $\theta_i$ . Thus for a given data set, the maximum value of  $P(\theta_i)$  is identified for all angles among all of the simulations; this single value can be used as the critical value for identifying significant patterns in all directions. It also potentially leads to a substantial decrease (a 180-fold reduction) in computation time; using this conservative shortcut, 100 replicate simulations yield the equivalent of 18000 replicates without its use. This approach should hold true for plots of any size and shape since the rescaling of counts by area removes the effect of shape on the marginal distribution of  $P(\theta_i)$ .

The use of this method is illustrated with a series of examples, ranging from random patterns to obvious patterns to obscure patterns, including both artificial

and field data sets. For all of these analyses, the space around each point was divided into  $1^\circ$  sectors, the wavelet scale ( $\omega_k$ ) ranged from  $1^\circ$  to  $45^\circ$ , and the French Top Hat wavelet was used as the windowing function  $g(x)$ . Direction was measured counter-clockwise from due east (i.e.  $0^\circ$  is east,  $90^\circ$  is north, etc.). Only points located in the middle 50% of the plot (as measured from the edges) were used as foci (this is conservative since the corner effect should only be a problem for the extreme corners). Significance levels were generated using 100 random replicates and averaging across all angles. All analyses were performed in the spatial statistics program *PASSAGE* (Rosenberg 2001).

## Results

### Artificial data

Three sets of simulated spatial patterns were used to illustrate the method: random patterns, obvious patterns, and obscure patterns. Fig. 3 presents the results of the analysis on two random point patterns, one consisting of 100 points, the other of 1000 points. As would be expected, the results indicate no directional bias;  $P(\theta_i)$  fluctuates randomly with direction and the magnitude of the peaks is well within the standard range found from other random simulations. Fig. 4 presents the results for three obvious and strong point patterns. Each of these plots consists of 1000 points; a fixed pattern with Gaussian error was set for each plot, with 20% of the points purely random. The method clearly indicates the

anisotropic pattern for every case. The pattern in Fig. 4c has a broader variance than those in Fig. 4a-b; this can be seen in both the relative breadth of pattern on the actual plotted maps, as well as the breadth of the peaks in the results of the wavelet analyses and the smaller overall variance (variances can be directly compared only when the plots are the same shape, scaled to the same area, and contain the same number of points).

The obscure patterns were simulated under very similar conditions. Each represents ten randomly placed parallel  $45^\circ$  (northeast/southwest) diagonal swaths of points (1000 total); the swaths have moderately large variances and heavily overlap, and are usually not clearly distinguishable. The difference among the plots is the percentage of points that were purely random and did not follow the set diagonal pattern: 10%, 20%, 33%, 50%, 67%, and 75%. The method is able to correctly identify the  $45^\circ$  trend in the cases with random points consisting of up to 50% of the plot (Fig. 5a-d). When 67% of the points are random (Fig. 5e), there is a barely significant peak at  $175^\circ$  and a slightly lower peak at  $45^\circ$ . Although no definitive pattern is indicated by this analysis (with more simulated replicates we would almost certainly be able to reject a pattern in this curve), the fact that virtually the entire curve exceeds the average values found from random simulated data indicates that there might be some very weak patterning in the data. This is in contrast to the case where 75% of the points were random (Fig. 5f) and the results are otherwise indistinguishable from the simulated data sets. These plots also reveal something of the stochastic nature of simulation; the data simulated with 50% of the points random (Fig. 5d) shows

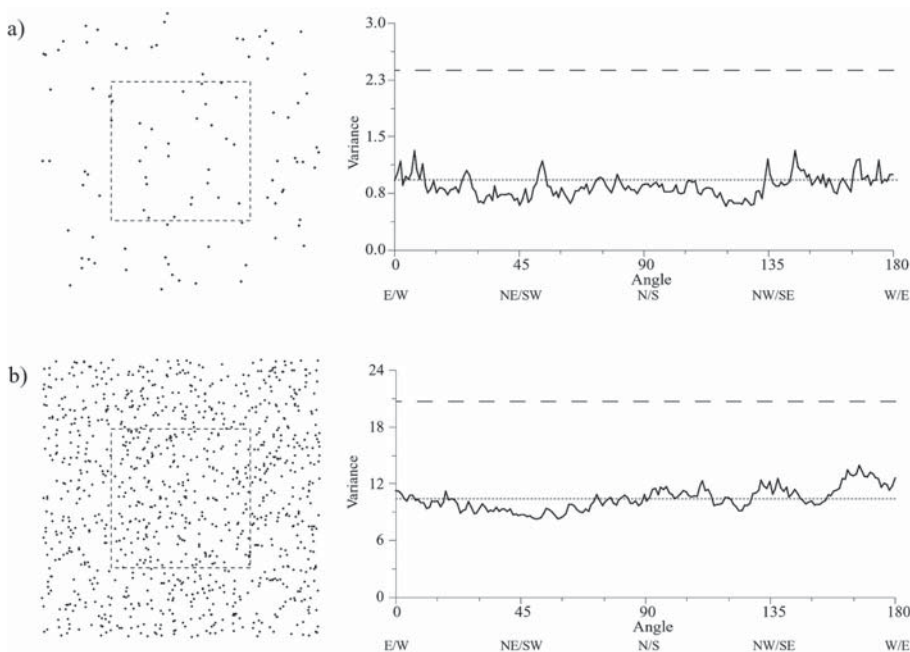


**Fig. 3.** Angular wavelet analysis of random point patterns. **a.** 100 points; **b.** 1000 points. Dotted squares outline the middle 50% of each plot and indicate points used as foci in the analysis. The long dashed line indicates the maximum peak found from 100 simulated random replicates; the dotted line the mean.

a stronger pattern (both visually and analytically) than the data simulated with only 33% of the points random (Fig. 5c).

*Field data*

The first field data set consists of a complete 1984 census of 4358 *Ambrosia dumosa* plants in a 1-ha (100 m × 100 m) plot from Joshua Tree National Park in California (Miriti et al. 1998), and has previously been used as an example in a number of spatial analyses (Miriti et al. 1998; Dungan et al. 2002; Perry et al. 2002). *A. dumosa* is an abundant, long-lived, drought deciduous shrub found on well-drained soils (Miriti et al. 1998). The study site was selected deliberately to minimize heterogeneity attributable to environmental variation. Previous work has shown small-scale clumping (Perry et al. 2002) and a significantly positive association between the locations of adult and juvenile plants (Miriti et al. 1998). Fig. 6a shows the study plot and the results of the angular wavelet analysis on this data. In the plot of the data, there appears to be some diagonal

streaking through the plot between 135° and 180°. These streaks have been noted in previous studies of these data, but were virtually unidentifiable by other anisotropic methods (Perry et al. 2002). The angular wavelet analysis clearly identifies the streaks by virtue of the large peak at 165° (Fig. 6a). It also identified a pattern around 15°, not clearly visible to the eye.

The second set of field data consists of 2015 isopod burrow locations collected by S. Citron-Pousty in the northern Negev Desert, Israel, in 1997. Burrow locations were exhaustively mapped over an irregular shaped 7.56-ha area. These data have been used as examples for other spatial analyses (Dungan et al. 2002). The pattern is clearly anisotropic (Fig. 6b), and although the pattern curves somewhat across the plot, most of the points are arrayed at roughly 45°. The method not only reveals this main trend, but also recognizes a kink in the pattern, with many points aligned somewhat more vertically, recognizable as the secondary small peak at 75°. These patterns reflect burrow alignment across three separate watersheds (S. Citron-Pousty pers. comm.).

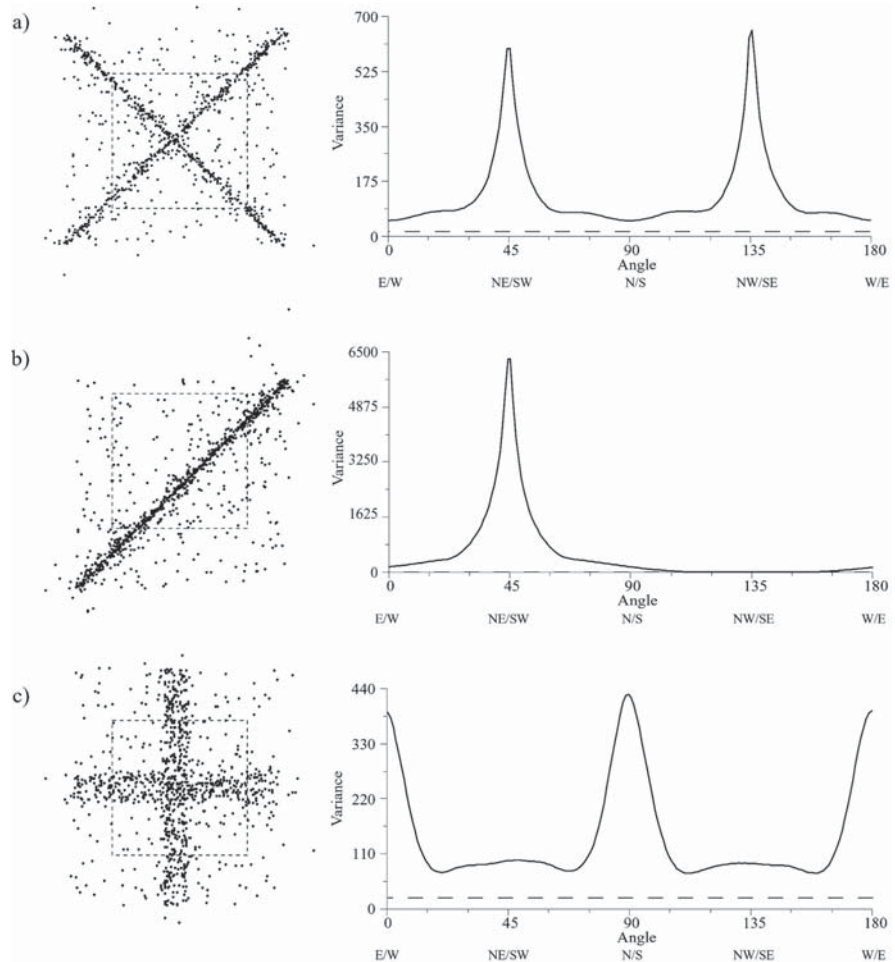


**Fig. 4.** Angular wavelet analysis of obvious point patterns. Each consists of 1000 points. Dotted squares outline the middle 50% of each plot and indicate points used as foci in the analysis. The long dashed line indicates the maximum peak found from 100 simulated random replicates.

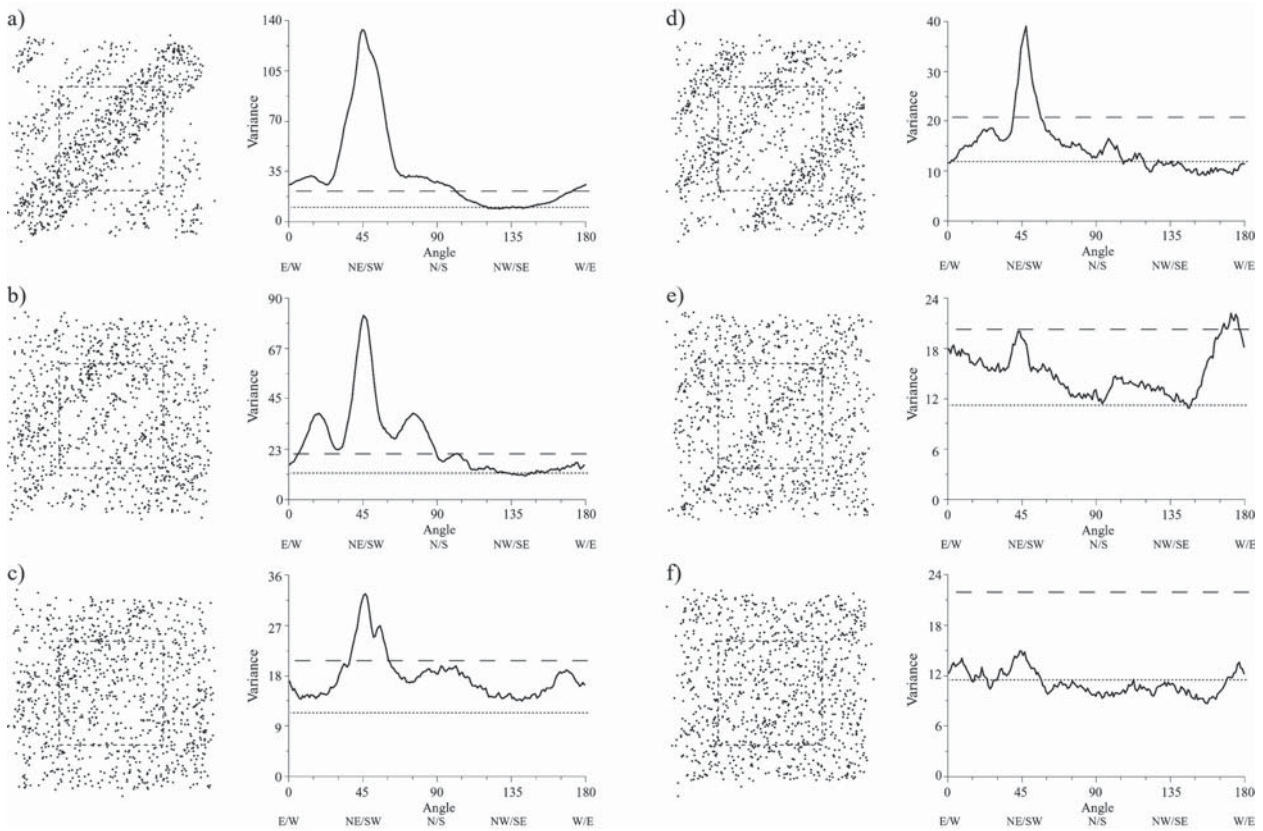


**Fig. 5.** Angular wavelet analysis of obscure point patterns. Each consists of 1 000 points in a general 45° trend. Each plot has a different percentage of points that are purely random: **a.** 10%; **b.** 20%; **c.** 33%; **d.** 50%; **e.** 67%; **f.** 75%. Dotted squares outline the middle 50% of each plot and indicate points used as foci in the analysis. The long dashed line indicates the maximum peak found from 100 simulated random replicates; the dotted line the mean.

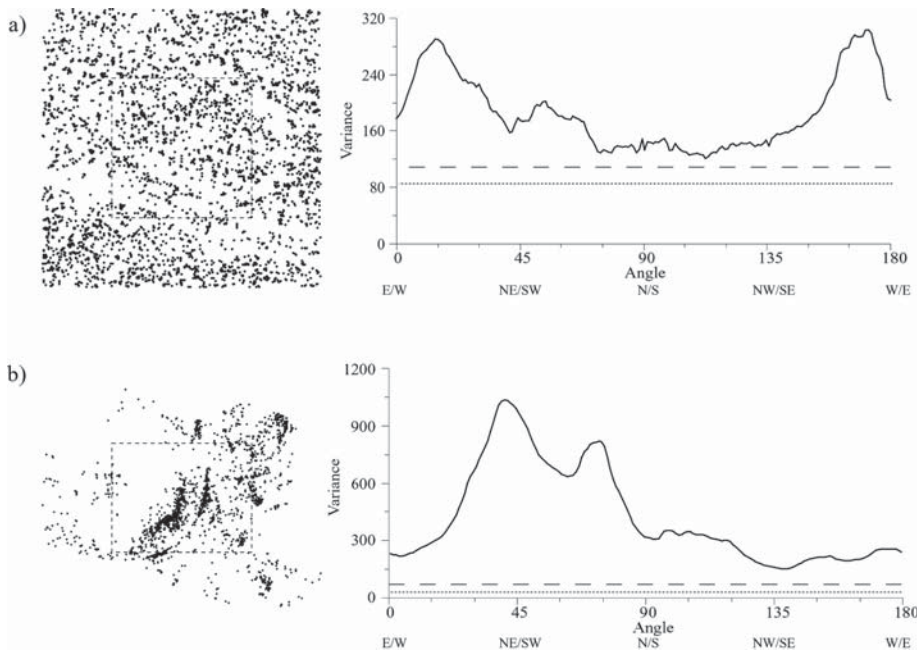


**Fig. 6.** Angular wavelet analysis of real data sets. **a.** Analysis of 4358 *Ambrosia dumosa* plants in a 1-ha square plot in California; **b.** Analysis of 2015 isopod burrows from the northern Negev Desert, Israel. Dotted rectangles outline the middle 50% of each plot and indicate points used as foci in the analysis. The long dashed line indicates the maximum peak found from 100 simulated random replicates; the dotted line the mean.

## Discussion

The angular wavelet analysis seems to be very good at identifying anisotropic patterns in point location data. Once the division of space around a focal point is used to create a circular transect, wavelet analysis is more suited for the analysis of anisotropy than other commonly used transect methods (e.g. blocked quadrat variance, paired quadrat variance, TTLQV, spectral analysis, etc.) because it is the only method which provides information on the location (in our case, direction) of pattern; the other methods only provide information on scale. Wavelet analysis should play a large role in ecological spatial analysis in the future because of its greater flexibility than more established methods. To some extent, wavelet analysis is more general than many classic transect methods because specific choice of the wavelet function will perform essentially the same analysis as these classic methods. For example, the  $V(b_k)$  plot from a French Top Hat wavelet is equivalent to 3TLQV (Dale & Mah 1998).

In most of the examples presented here, the anisotropic pattern in the data was obvious from a simple inspection of a point plot, and it could be argued that an elaborate method for the identification of anisotropy is unnecessary. While this is true for many patterns (e.g. Figs. 4, 5a-d, and 6b), trends can be much more subtle in others (e.g. Fig. 6a). Humans are notoriously bad at distinguishing randomness in a pattern; manual construction of a 'random' pattern almost always leads to significant regularity among points (pers. obs.). However, no method should ever completely replace the visual inspection of one's data and the importance and utility of mapping and simple summary statistics as a first step in any spatial analysis cannot be overemphasized (Korie et al. 1998; Perry et al. 2002).

Spatial analysis is traditionally global: the spatial pattern is analysed across the entire extent of the data. In recent years there has been a surge of interest in local spatial analysis: spatial pattern analysed for specific locations within the study area which apply only to those locations (Anselin 1995; Getis & Ord 1995; Ord & Getis 1995; Sokal et al. 1998a,b). The method presented here easily allows for local analysis, simply by retaining the wavelet analysis for an individual focal point rather than averaging over all points.

Distances among points play no role in the described analyses. Distance information could easily be incorporated into the analysis by only counting points within a certain range of the focal point. This could be used to restrict the analysis to a smaller range, or could be repeated for a series of distance classes (e.g. 0-5 m, 5-10 m, 15-20 m, etc.) the way is commonly done in correlogram or variogram analysis (Sokal & Oden 1978;

Cliff & Ord 1981; Isaaks & Srivastava 1989). This could allow one to tease apart scale effects, since local (short distance) patterns need not be identical to global (long distance) patterns (Dungan et al. 2002; Perry et al. 2002).

This method has been described for analysis of univariate patterns. Multivariate point pattern analysis (e.g. analysing the relative spatial distribution of two plant species) is another strong area of interest in ecology. Many existing point pattern analysis methods can easily be adapted to multivariate data (Dale 1999; Dale et al. 2002), including some of those for anisotropy (e.g. Haase 2001). The current method could also clearly be adapted to multivariate data by repeating the analysis such that only points of a specific type are used as foci and only points of a different type (for example) are counted within the sectors.

**Acknowledgements.** I wish to thank Mark Dale and anonymous reviewers for advice on early versions of this manuscript, and M. Miriti and S. Citron-Pousty for the gracious use of their data.

## References

- Anselin, L. 1995. Local indicators of spatial association – LISA. *Geogr. Anal.* 27: 93-115.
- Bradshaw, G.A. & McIntosh, B.A. 1994. Detecting climate-induced patterns using wavelet analysis. *Environ. Pollut.* 83: 135-142.
- Bradshaw, G.A. & Spies, T.A. 1992. Characterizing canopy gap structure in forests using wavelet analysis. *J. Ecol.* 80: 205-215.
- Chui, C.K. 1992. *An introduction to wavelets. Wavelet analysis and its applications, Vol. 1.* Academic Press, San Diego, CA, US.
- Cliff, A.D. & Ord, J.K. 1981. *Spatial processes.* Pion, London, UK.
- Dale, M.R.T. 1999. *Spatial pattern analysis in plant ecology.* Cambridge University Press, Cambridge, UK.
- Dale, M.R.T. & Mah, M. 1998. The use of wavelets for spatial pattern analysis in ecology. *J. Veg. Sci.* 9: 805-814.
- Dale, M.R.T., Dixon, P.M., Fortin, M.-J., Legendre, P., Myers, D.E. & Rosenberg, M.S. 2002. Conceptual and mathematical relationships among methods for spatial analysis. *Ecography* 25: 558-577.
- Daubechies, I. 1988. Orthonormal bases of compactly supported wavelets. *Comm. Pure Appl. Math.* 41: 909-996.
- Daubechies, I. 1993. Wavelet transforms and orthonormal wavelet bases. In: Daubechies, I. (ed.) *Different perspectives on wavelets*, pp. 173-205, American Mathematical Society, Providence, RI, US.
- Daubechies, I., Grossman, A. & Meyer, Y.J. 1986. Painless non-orthogonal expansions. *J. Math. Phys.* 27: 1271-1283.
- Diggle, P.J. 1983. *Statistical analysis of spatial point patterns.*

- Academic Press, London, UK.
- Donoho, D.L. 1993. Nonlinear wavelet methods for recovery of signals, densities, and spectra from indirect and noisy data. In: Daubechies, I. (ed.) *Different perspectives on wavelets*, pp. 173-205, American Mathematical Society, Providence, RI, US.
- Dungan, J.L., Perry, J.N., Dale, M.R.T., Legendre, P., Citron-Pousty, S., Fortin, M.-J., Jakomulska, A., Miriti, M.N. & Rosenberg, M.S. 2002. A balanced view of scaling in spatial statistical analysis. *Ecography* 25: 626-640.
- Falsetti, A.B. & Sokal, R.R. 1993. Genetic structure of human populations in the British Isles. *Ann. Hum. Biol.* 20: 215-229.
- Franklin, J., Michaelsen, J. & Strahler, A.H. 1985. Spatial-analysis of density dependent pattern in coniferous forest stands. *Vegetatio* 64: 29-36.
- Getis, A. & Ord, J.K. 1995. The analysis of spatial association by use of distance statistics. *Geogr. Anal.* 24: 189-206.
- Greiner, M., Lipa, P. & Carruthers, P. 1996. Wavelets: Some applications in physics. *Complexity* 2: 31-36.
- Haase, P. 1995. Spatial pattern analysis in ecology based on Ripley's K-function: Introduction and methods of edge correction. *J. Veg. Sci.* 6: 575-582.
- Haase, P. 2001. Can isotropy vs. anisotropy in the spatial association of plant species reveal physical vs. biotic facilitation? *J. Veg. Sci.* 12: 127-136.
- Haining, R. 1982. Describing and modeling rural settlement maps. *Ann. Ass. Am. Geogr.* 72: 211-223.
- Hill, M.O. 1973. The intensity of spatial pattern in plant communities. *J. Ecol.* 61: 225-235.
- Isaaks, E.H. & Srivastava, R.M. 1989. *An introduction to applied geostatistics*. Oxford University Press, Oxford, UK.
- Korie, S., Clark, S.J., Perry, J.N., Mugglestone, M.A., Bartlett, P.W., Marshall, E.J.P. & Mann, J.A. 1998. Analysing maps of dispersal around a single focus (with Discussion). *Ecol. Environ. Stat.* 5: 317-350.
- Miriti, M.N., Howe, H.F. & Wright, S.J. 1998. Spatial patterns of mortality in a Colorado desert plant community. *Plant Ecol.* 136: 41-51.
- Mugglestone, M.A. & Renshaw, E. 1996. A practical guide to the spectral analysis of spatial point processes. *Comput. Stat. Data Anal.* 21: 43-65.
- Nakken, M. 1999. Wavelet analysis of rainfall-runoff variability isolating climatic from anthropogenic patterns. *Environ. Model. Software* 14: 283-295.
- Oden, N.L. & Sokal, R.R. 1986. Directional autocorrelation: An extension of spatial correlograms to two dimensions. *Syst. Zool.* 35: 608-617.
- Ord, J.K. & Getis, A. 1995. Local spatial autocorrelation statistics: Distributional issues and application. *Geogr. Anal.* 27: 286-306.
- Perry, J.N. 1995. Spatial analysis by distance indices. *J. Anim. Ecol.* 64: 303-314.
- Perry, J.N., Winder, L., Holland, J.M. & Alston, R.D. 1999. Red-blue plots for detecting clusters in count data. *Ecol. Lett.* 2: 106-113.
- Perry, J.N., Liebhold, A.M., Rosenberg, M.S., Dungan, J.L., Miriti, M.N., Jakomulska, A. & Citron-Pousty, S. 2002. Illustration and guidelines for selecting statistical methods for quantifying spatial patterns in ecological data. *Ecography* 25: 578-600.
- Ripley, B.D. 1976. The second-order analysis of stationary point processes. *J. Appl. Probab.* 13: 255-266.
- Ripley, B.D. 1977. Modelling spatial patterns. *J. R. Stat. Soc. B* 39: 172-212.
- Ripley, B.D. 1979. Tests of randomness for spatial point patterns. *J. R. Stat. Soc. B* 41: 368-374.
- Rosenberg, M.S. 2000. The bearing correlogram: A new method of analysing directional spatial autocorrelation. *Geogr. Anal.* 32: 267-278.
- Rosenberg, M.S. 2001. *PASSAGE. Pattern analysis, spatial statistics, and geographic exegesis*. <http://lweb.la.asu.edu/rosenberg/Passage>.
- Simon, G. 1997. An angular version of spatial correlations, with exact significance tests. *Geogr. Anal.* 29: 267-278.
- Sokal, R.R. & Oden, N.L. 1978. Spatial autocorrelation in biology 1. Methodology. *Biol. J. Linn. Soc.* 10: 199-228.
- Sokal, R.R., Oden, N.L. & Thomson, B.A. 1998a. Local spatial autocorrelation in a biological model. *Geogr. Anal.* 30: 331-354.
- Sokal, R.R., Oden, N.L. & Thomson, B.A. 1998b. Local spatial autocorrelation in biological variables. *Biol. J. Linn. Soc.* 65: 41-62.
- Strang, G. 1994. Wavelets. *Am. Sci.* 82: 250-255.
- Upton, G.J.G. & Fingleton, B. 1985. *Spatial data analysis by example. Vol. 1: Point pattern and quantitative data*. Wiley, Chichester, UK.

Received 10 July 2003;

Accepted 16 November 2003;

Co-ordinating Editor: N. Kenkel.